ELSEVIER

Journal of Photochemistry and Photobiology A: Chemistry 141 (2001) 247–254

Journal of Photochemistry and Photobiology A:Chemistry

www.elsevier.nl/locate/jphotochem

Photochemical and heterogeneous photocatalytic degradation of waste vinylsulphone dyes: a case study with hydrolysed Reactive Black 5

Idil Arslan Alaton, Işil Akmehmet Balcioglu*

Institute of Environmental Sciences, Bogaziçi University, 80815 Bebek-Istanbul, Turkey

Received 21 February 2001; received in revised form 12 March 2001; accepted 10 April 2001

Abstract

Aqueous solutions of hydrolyzed Reactive Black 5 (RB5) dye, a well-known surrogate for non-biodegradable azo dyes, were photochemically and photocatalytically treated by employing the H_2O_2/UV-C and TiO_2/UV-A advanced oxidation systems, respectively. The observed effects of reaction pH, oxidant dose and initial dyestuff concentration were used to explain the $OH^\bullet$ induced color disappearance kinetics empirically. Accordingly, the waste dyestuff solutions could be completely decolorised ($k_{d,max} = 0.155\,min^{-1}$; H_2O_2/UV-C system) and effectively mineralised ($k_{TOC,max} = 0.01\,min^{-1}$; H_2O_2/UV-C system), with an average overall TOC removal of 78% after 120 min advanced oxidation at the specified optimised reaction conditions. The treatment via H_2O_2/UV-C was mainly governed by $OH^\bullet$ type oxidation rather than direct UV-C or UV-A photolysis, and the bleaching effect of the TiO_2/UV-A process could be successfully fitted to the empirical Langmuir–Hinshelwood (L–H) kinetic model ($k_{L-H} = 4.47\,mg\,l^{-1}\,min^{-1}$; $K_{L-H} = 2.01\,l\,mg^{-1}$).

Keywords: Textile dyestuffs; Reactive Black 5; Advanced oxidation processes (AOPs); H_2O_2/UV-C treatment; TiO_2/UV-A treatment; Langmuir–Hinshelwood type kinetic equation

1. Introduction

In the last few decades, dyestuffs and allied industries have become subject to increasingly stringent regulations designed to protect the human health and environment. As a consequence, the effective elimination of colored effluents originating from the textile and related industries has become an important problem to the textile dyer and finisher as to meet the new discharge limit values [1]. The most common methods employed to treat wastewater containing organic dyes and pigments are classifiable into three main categories [2]: physical (adsorption, filtration, flotation), chemical (coagulation, oxidation, reduction, electrolysis) and biological (aerobic, anaerobic degradation). However, due to the complexity and variety of dyestuffs employed in the textile dyeing process, it has become rather difficult to find a unique treatment procedure that covers the effective elimination of all dye types and classes. Particularly, biochemical oxidation suffers from significant limitations since most dyestuffs found in the commercial market have been intentionally designed to resist aerobic microbial degradation [3]. Consequently, most dyestuffs are of a rather recalcitrant nature and have to be treated by alternative advanced physicochemical processes.

Homogenous advanced oxidation via combinations of H_2O_2, O_3 and UV-C light is one of the principal and most effective methods for decomposing water-soluble organic pollutants found in water and wastewater [4–8] and their application to reactive dyestuffs has already been investigated by many researchers recently [9–13]. Hydrogen peroxide alone does not oxidize more difficult to degrade dyestuffs, however, it can be activated to form highly reactive species, mainly hydroxyl radicals ($OH^\bullet$) by means of adding soluble ferrous ion salt to an acidic solution of H_2O_2 producing the Fenton's reagent, ozone at high pH, or in the presence of UV-C ($300\,nm > \lambda > 200\,nm$) light irradiation [14]. In fact, H_2O_2/UV-C is one of the most widely examined wastewater treatment methods together with the Fenton's oxidation [15–17]. H_2O_2/UV-C offers several advantages over the ferrous iron catalyzed oxidation as this oxidation system is not restricted to acidic pH (<3.0) and the absence of ferric iron sludge that otherwise has to be eliminated by a costly pH-neutralization and filtration procedure [10].

On the other hand, TiO_2-mediated heterogeneous photocatalytic treatment makes use of the UV-A (400 nm >

* Corresponding author. Tel.: +90-212-263-15-40; fax: +90-212-257-50-33.
E-mail address: balciogl@boun.edu.tr (I.A. Balcioglu).

1010-6030/01/$ – see front matter
PII: S1010-6030(01)00440-3

$\lambda > 300$ nm) fraction of solar irradiation to produce $OH^{\bullet}$ [18]. TiO_2, which has a suitable bandgap energy (3.2 eV), is stable, inexpensive and has a rather high photoactivity. The principal advantage of the TiO_2/UV-A system over homogenous advanced oxidation processes (AOPs) is its relative robustness to reaction conditions. Homogeneous photochemical and TiO_2-mediated heterogeneous photocatalytic treatment of various organic and inorganic model pollutants has been extensively reported in the recent scientific literature [14,19]. However, the effectiveness of AOPs in decomposing commercial reactive azo dyes as well as their competitiveness in terms of operating costs need still to be further questioned, in particular for the heterogeneous photocatalytic treatment process due to its outstandingly high operational cost and complexity.

Furthermore, though it has been already demonstrated that AOPs can be effectively applied for the degradation of textile dyes in numerous previous studies, nearly all of which have concentrated on the color (reactant) disappearance kinetics, it is the ultimate oxidation of TOC content of the dyestuffs that has to be considered for the full scale applications of AOPs. Indeed, TOC destruction is the ultimate goal of AOPs, and thus, its removal deserves utmost significance. With the aim to contribute to the clarification of the above mentioned facts, the present study aimed to comparatively evaluate the efficiency of applying a photochemical (H_2O_2/UV-C) and a heterogeneous photocatalytic (TiO_2/UV-A) treatment system for degradation of a common reactive disazo type dyestuff, hydrolyzed Reactive Black 5 (RB5). This dye was chosen as a representative refractory chemical due to its relatively high consumption rate (e.g. the annual consumption of RB5 sold under the trade name Remazol Black B is 1000 metric tonnes in Turkey) for reactive dyeing [20] as well as the fact that up to 50% of fiber reactive dyes (typically 20%) remain in the exhausted (spent) dyebath in its hydrolyzed form and cannot be recovered [21].

2. Experimental

2.1. Materials

The vinylsulphone disazo dye C.I. RB5 (Remazol Black B dyestuff preparation, $C_{26}H_{21}O_{19}N_5S_6Na_4$, molecular weight = 991.8, average purity = 82.5%) was kindly supplied by DyStar, Turkey. To obtain a fully hydrolyzed reactive dye solution, 1000 mg l^{-1} aqueous stock solution of the dye was prepared by first dissolving the dye in distilled de-ionized water and then adding 4.5 g l^{-1} from 48°C Bé NaOH solution under thermostatically controlled (60°C) continuous stirring for at least 4 h. Thereafter, the prepared "waste" dye solution was kept for 24 h to ensure complete hydrolysis.

As determined spectrophotometrically, the visible absorption band remained invariant in the pH range 2.0–10.5 and increasing the pH to above 10.5 resulted in the bathochromic shift of the characteristic absorption band of RB5 in the visible spectrum from 597 to 613 nm ($10.5 < pH < 11.5$) and finally to 620 nm at pH 12. Concomitantly, the addition of alkali resulted in the 1,2-elimination of the alkali-sensitive sulphatoethylsulphone precursor to release the reactive vinylsulphone system [22]. The origin of this shift in the absorption maximum lies in the ionization of the hydrazone section of the chromophoric group at high pH-values. At pH 10.5, the characteristic absorption band at 227 nm completely vanished and the absorption band in the near-UV spectral region shifted from 310 to 318 nm, whereas increasing the pH to >12 resulted in the complete disappearance of the 392 nm peak, that remained invariant at a $pH < 12$.

The P25 TiO_2 powder supplied by Degussa Corporation, with an average particle size of 30 nm, a mean BET surface area of 50 m^2 g^{-1} and a 70% anatase–30% rutile crystal phase, was used without further purification. The oxidant H_2O_2 (30%, w/w stock solution) was purchased from Merck. Necessary pH adjustments were made with diluted HCl and NaOH solutions. All other materials used for chemical analyses were reagent grade.

2.2. The photochemical reactor

H_2O_2/UV-C oxidation of hydrolyzed RB5 solution was conducted for 2 h in a 2.5 l capacity annular photoreactor at batch mode. The UV-C reactor was equipped with a 25 W low pressure mercury vapor UV-C lamp ($L = 45$ cm; $d = 2.5$ cm) that mainly emitted at $\lambda = 254$ nm and was placed into a quartz envelope. The incident light flux of the UV-C lamp was determined by hydrogen peroxide actinometry [23] as $I_o = 2.02 \times 10^{-5}$ Einstein l^{-1} s^{-1} and the effective path length in the photochemical reactor was calculated as $d = 1.72$ cm from the direct UV-C photolysis of a H_2O_2 aqueous solution at low concentration (10^{-4} M) as described by Nicole et al. [23]. Mixing was provided by circulating the reaction solution with a peristaltic pump (Cole Parmer) at a rate of 150 ml min^{-1}.

2.3. The photocatalytic reactor

Heterogeneous photocatalytic (TiO_2/UV-A) treatment of the hydrolyzed RB5 solution was performed in a 1 l capacity annular batch borosilicate glass reactor presented elsewhere [17]. A 20 W black light fluorescent lamp (General Electric) was placed at the center of the photocatalytic reactor as the UV-A light source. The reaction solution was stirred by both recirculation of the slurry with a Cole Parmer peristaltic pump and purging air at a flow rate of 400 ml min^{-1} through two sintered glass discs placed at the reactor bottom. The light intensity of the UV-A light source was measured by employing ferrioxalate actinometry as 9.17×10^{-7} Einstein l^{-1} s^{-1} [24].

Table 1
Molar extinction coefficients at λ_{max} ($\varepsilon_{\lambda_{max}}$) and at 254 nm ($\varepsilon_{254}$) for RB5 ($C_{dye}$ = 20–200 mg l^{-1}) at varying pH and for H_2O_2

Conditions	$\varepsilon_{\lambda_{max}}$ (M^{-1} cm^{-1})	$\varepsilon_{UV_{254}}$ (M^{-1} cm^{-1})
pH 4.95[a]	14565	7364
pH 4.95[b]	14074	7528
pH 10.5[b]	14606	7446
pH 11.0[b]	14646	7773
pH 12.5 (hydrolyzed)[c]	15219	8182
H_2O_2	–	17

[a] Natural pH of RB5.
[b] pH was re-adjusted to obtain a fully hydrolyzed reactive dye solutions.
[c] λ_{max} shifts to 620 nm wavelength.

2.4. Methodology

A volume of 10 ml aliquots of raw and treated samples were taken from the corresponding reactors at regular time intervals and immediately analyzed for color, COD and TOC. During the H_2O_2/UV-C experiments residual (unreacted) H_2O_2 in the samples was destroyed with the enzyme catalase (made from *Micrococcus lysodeikticus*; contains 176 340 activity units (AU) per ml; 1 AU destroys 1 mmol of H_2O_2 per minute at pH 7 and 25°C) immediately after sampling to quench the reaction and prevent any interference with the analytical measurements. Photocatalytically treated aliquots were first filtered through Millipore membranes (cut-off = 0.45 μm) to remove TiO_2 powder from the samples. The visible light absorption band at the characteristic wavelength of RB5 (Table 1) was recorded with a Shimadzu UV-160 model UV–VIS spectrophotometer to follow up the progress of decolorization..

The COD of the samples was determined according to the closed reflux, colorimetric method [25]. The extend of mineralization of the reaction samples was monitored by a TCM-480 model total organic carbon analyzer (Carlo Erba, Fisons Instruments).

2.5. Application of global kinetic equations

To compare the decolorization, oxidation, and mineralization rates at varying reaction conditions of the investigated AOPs, global rate laws were used to determine the pseudo-first order rate constants for $A_{\lambda_{max}}$, COD and TOC, respectively. These abatement rate constants were calculated using the formulae:

$$\ln\left(\frac{A_{\lambda_{max}}}{A_{\lambda_{max,0}}}\right) = k_d t \quad (1)$$

with

$$k_d = k_{OH^\bullet,dye}[OH^\bullet] \quad (2)$$

where k_d is the pseudo-first order decolorization rate constant, $k_{OH^\bullet,dye}$ the actual reaction rate constant between the dyestuff and $OH^\bullet$ the molar concentration of hydroxyl radicals that are assumed to remain constant throughout the course of experiments,. Analogously, the pseudo-first order rate constants, k_{COD} and k_{TOC}, can be calculated for COD and TOC removal, respectively.

3. Results and discussion

3.1. Dye degradation by H_2O_2/UV-C treatment

3.1.1. Decomposition by direct UV-C photolysis and single oxidant addition

A previous set of control experiments using 10 mM H_2O_2 alone at pH 7 was conducted, but no RB5 degradation (C_o = 75 mg l^{-1}) was obtained with this oxidant (not shown data). Therefore, it can be concluded that the oxidizing power of H_2O_2 is not sufficient to bring about RB5 decomposition. To examine the effect of UV-C light on RB5 degradation in the absence of H_2O_2, a separate experiment was also carried out at pH 7. As can be seen later in Fig. 2a, only a slight bleaching effect ($k_d = 6 \times 10^{-3}$ min^{-1}) could be achieved by employing UV-C light irradiation, whereas no reduction in COD and TOC was observed throughout the selected reaction period. Since the reaction mechanism for direct UV-C photolysis of organic compounds is of a rather complex nature, it can be speculated that during UV-C light exposure an electronically excited state of the dye was generated, where RB5 might undergo intermolecular transformations, however, further decomposition of excited molecules to radicals and/or oxidized species did not occur.

Certain dyes can be photo-decolorized in the presence of UV-C light irradiation. Chu and Ma [26] found that direct UV-C photolysis of several azo and anthraquinone dyes followed a pseudo-first order decay. From the observations of the present study in can be inferred that RB5 is photolytically very stable and its degradation necessitates the application of H_2O_2 catalyzed UV-C photolysis at appropriate H_2O_2 doses.

3.1.2. Effect of pH

H_2O_2/UV-C oxidation of 75 mg l^{-1} hydrolyzed RB5 was carried out in the photochemical reactor for 2 h at varying pH (2.5, 7.0 and 11.5) and an initial H_2O_2 dose of 10 mM (340 mg l^{-1}). Fig. 1 presents the k_d-values and overall percent COD and TOC removal efficiencies obtained for 10 mM H_2O_2/UV-C treatment at different pH-values.

According to the figure, changing the reaction pH did not affect the treatment performance of the H_2O_2/UV-C process seriously. The slight increase in overall percent COD and TOC removal efficiencies was rather insignificant, and from the above figure a minor tendency of increasing k_d (found as 0.145 min^{-1} at pH 2.5 and as 0.182 min^{-1} at pH 11.5) with increasing pH is evident.

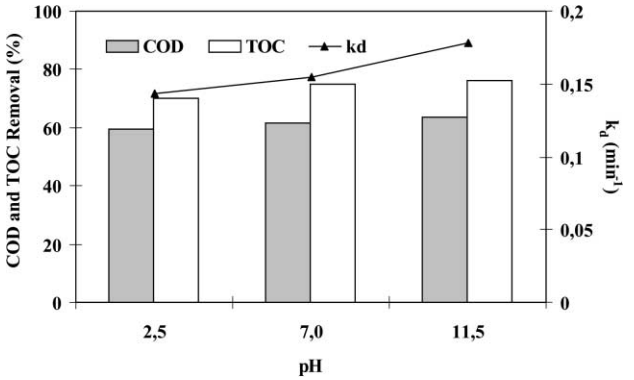

Fig. 1. Changes in k_d-values, overall percent COD and TOC removal efficiencies obtained for 10 mM H_2O_2/UV-C oxidation of 75 mg l^{-1} waste RB5 in the photochemical reactor as a function of pH.

3.1.3. Effect of initial oxidant dose

The effect of varying the initial H_2O_2 dose (0, 5, 10, 25 and 50 mM) at pH 7 on color, COD and TOC abatement kinetics was also examined for 75 mg l^{-1} RB5 and results are displayed in Fig. 2a–c.

The applied H_2O_2 dose significantly affected the H_2O_2/UV-C oxidation rates. The removal rates increased considerably with increasing the initial H_2O_2 concentration from 0 to 10 mM. However, while the oxidant dose was increased gradually to a certain limit, dye degradation rates changed only slightly reaching a maximum value at a H_2O_2 dose of around 10 mM ($k_d = 0.155\,min^{-1}$). Elevating the H_2O_2 concentration from 10 to 25 mM even slightly decreased the color, COD and TOC removal rates and further increase in the applied H_2O_2 dose to 50 mM caused a significant inhibition of the H_2O_2/UV-C process performance. Similar trends for the effect of varying initial H_2O_2 concentration on pseudo-first order decolorization rate constants k_d were observed in former investigations conducted with fiber reactive [13] and acid dyes [27]. The above mentioned observations are not unusual for H_2O_2/UV-C oxidation systems, since it is already well established that H_2O_2 itself acts as an effective OH$^\bullet$ scavenger at concentrations that are specific for the pollutant in question. This observation is in accordance with the following empirical equation [28]:

$$H_2O_2 + OH^\bullet \rightarrow HO_2^\bullet + H_2O;\quad k = (1.2\text{–}4.5) \times 10^7\,M^{-1}\,s^{-1} \qquad (3)$$

Although $HO_2^\bullet$ promotes radical chain reactions and is an effective oxidant itself, its oxidation potential is much lower than that of OH$^\bullet$. Thus, as stated in many other experimental investigations, the presence of excess H_2O_2 can lower the treatment efficiency of AOPs and it is very important to optimize the applied H_2O_2 dose to maximize the treatment performance of the AOP.

Fig. 2b and c also delineates that the rate of disappearance of the reactant (i.e. decolorization) is noticeably faster than that of COD and TOC. Particularly, COD reduction leveled off within the first 30–40 min of H_2O_2/UV-C treatment for all H_2O_2 doses above 5 mM, whereas the TOC abatement continued until the end of the selected treatment period.

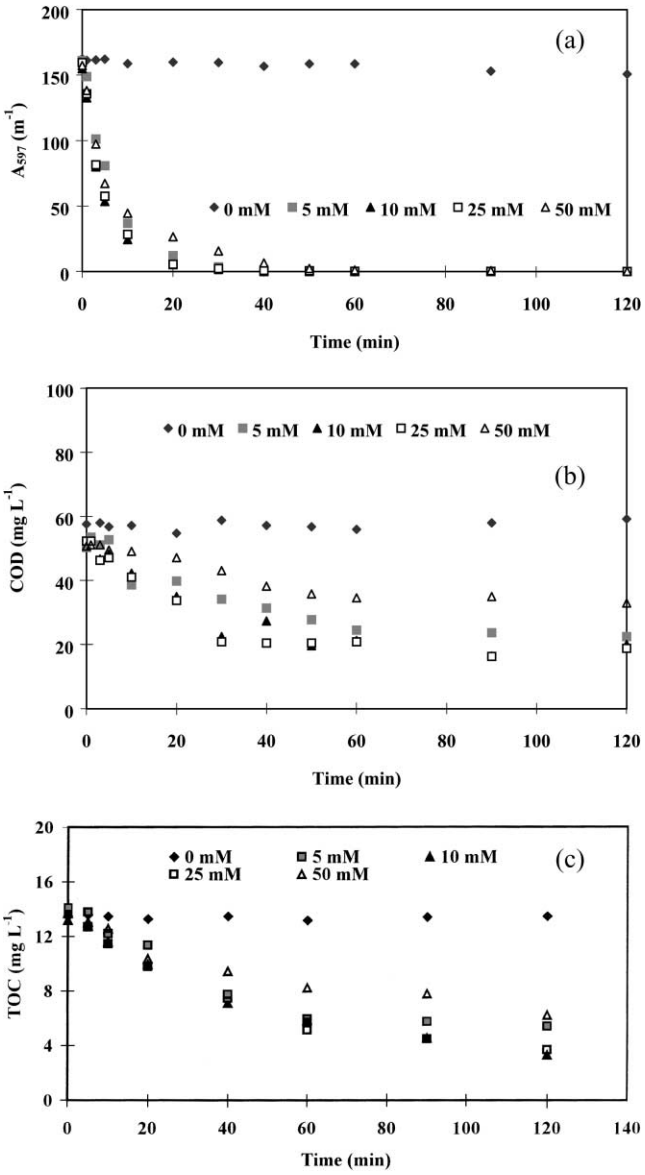

Fig. 2. Time-dependent changes in color (a), COD (b) and TOC (c) during H_2O_2/UV-C oxidation of 75 mg l^{-1} waste RB5 in the photochemical reactor at pH 7.

Fig. 3 presents k_d-values together with percent total COD and TOC removal efficiencies observed for the H_2O_2/UV-C treatment of 75 mg l^{-1} RB5 at pH 7 and varying H_2O_2 doses. Generally spoken, the figure implies that the existence of an optimum initial H_2O_2 dose was observed for all investigated environmental parameters.

Table 2 summarizes obtained pseudo-first order removal rates (k_{app}) relative to the k_d-values ($k_{app}k_d^{-1}$) and overall percent removal efficiencies in terms of the investigated environmental sum parameters for H_2O_2/UV-C treatment of 75 mg l^{-1} RB5 in the presence of 10 mM H_2O_2 at pH 7.

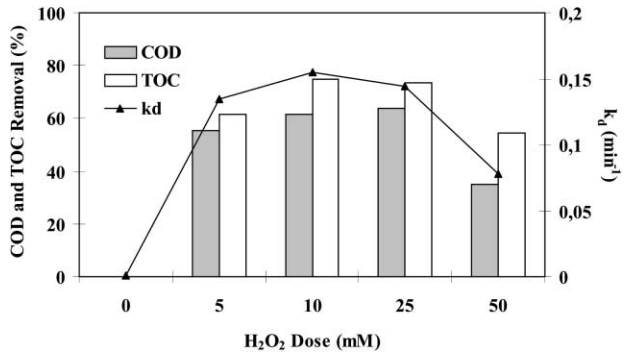

Fig. 3. Changes in k_d-values, overall percent COD and TOC removal efficiencies obtained for H_2O_2/UV-C oxidation of 75 mg l^{-1} waste RB5 in the photochemical reactor at pH 7 as a function of initial H_2O_2 dose.

From Table 2 it is evident that the rate of oxidation and mineralization of RB5 proceeded considerably slow as compared to the initial electrophilic cleavage of its chromophoric groupings (i.e. –N=N– bonds and attached phenolic moieties) that cause a rapid decolorization. This phenomenon and the fact that in particular COD removal levels off in the second part of the experiments, is attributable to the formation of advanced oxidation products (i.e. aldehydes, ketones and organic acids) being less amenable to $OH^{\bullet}$ attack [29,30]. Moreover, it has been postulated that AOPs may produce rate-controlling, refractory intermediates that can control or at least limit COD and TOC abatement kinetics [31].

3.2. Dye degradation by TiO_2/UV-A treatment

Heterogeneous photocatalytic oxidation experiments with RB5 were conducted in the photocatalytic reactor for 2 h in 1 g l^{-1} suspensions of TiO_2 at varying (1) reaction pHs (4.0, 7.0 and 11.0) and (2) initial waste RB5 concentrations (25–150 mg l^{-1}). It should be also noted here that the blank experiments conducted in the presence of UV-A radiation, but in the absence of the semiconductor did not result in any measurable degradation of waste RB5 (not shown data).

3.2.1. Dark adsorption tests

RB5 (75 mg l^{-1}) solution was treated for 2 h at pH 4 in photocatalytic reactor in the absence of UV-A light irradiation to assess the extend of initial dark adsorption of the azo dye and to permit adsorption–desorption equilibrium to be reached on the photocatalyst surface. In that dark control experiment, 27.7% color, 35.4% COD and 32.7% TOC were removed as a consequence of the electrostatic interaction (repulsion) between the positively charged TiO_2 surface ($TiO_{2_{ZPC}} = 6.3$) [32] and the reactive dye anions at the investigated pH. Pre-equilibration adsorption of 75 mg l^{-1} RB5 was achieved after 80 min dark treatment in the photocatalytic reactor. Different concentrations of dye solutions were equilibrated for this predetermined time in the absence of UV-A light irradiation to achieve a steady state dye concentration prior to the photocatalytic experiments.

To assess adsorption characteristics of RB5 in more detail, 100 ml 75 mg l^{-1} solutions were treated for 24 h at five concentrations of the photocatalyst (0, 0.25, 0.50, 0.75, 1.0 and 2.0 g l^{-1}) at pH 4 and room temperature (20°C) in a mechanical shaker. The extend of adsorption of the azo dye on TiO_2 was evaluated in terms of color removal rate (absorbance at 597 nm, A_{597}). Data obtained from the adsorption experiments of RB5 were fitted to the modified empirical Langmuir equation [33]:

$$\frac{A_{597,e}}{y} = \frac{1}{Ky_m} + \frac{A_{597,e}}{y_m} \quad (4)$$

where $A_{597,e}$ is the equilibrium absorbance of RB5 at 597 nm after 24 h adsorption, y represents the ratio of equilibrium absorbance of the dye to the mass of TiO_2 adsorbent, whereas the constants K and y_m are corresponding to the adsorption constant and the ratio of equilibrium absorbance of the dye to the mass of TiO_2 adsorbent for complete monolayer adsorption (i.e. maximum adsorption), respectively.

The dimensionless separation factor (R_L) indicates the shape of the Langmuir isotherm to be either favorable ($0 < R_L < 1$), unfavorable ($R_L > 1$), linear ($R_L = 1$), or irreversible ($R_L = 0$):

$$R_L = \frac{1}{1 + KA_{597,0}} \quad (5)$$

with $A_{597,0}$ being the initial absorbance of the highest concentration investigated in the dark adsorption experiments.

Fig. 4 presents the $A_{597,0}/y$ versus $A_{597,0}$ plot together with the obtained Langmuir parameters y_m, which is the maxi-

Table 2
Relative pseudo-first order removal rate constants and overall percent COD and TOC removal efficiencies for 2 h H_2O_2 (10 mM)/UV-C treatment of 75 mg l^{-1} hydrolyzed RB5 at pH 7

Process parameter	$k_{app}k_d^{-1}$	Removal (%)
$A_{\lambda_{max}}$	1.000	100
COD	0.125	62
TOC	0.063	75

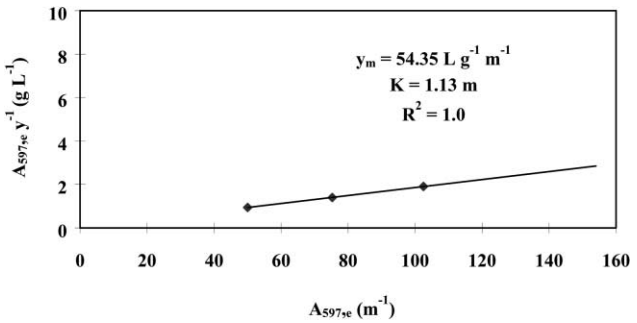

Fig. 4. Establishment of the Langmuir monolayer adsorption constants for waste RB5 at pH 4.

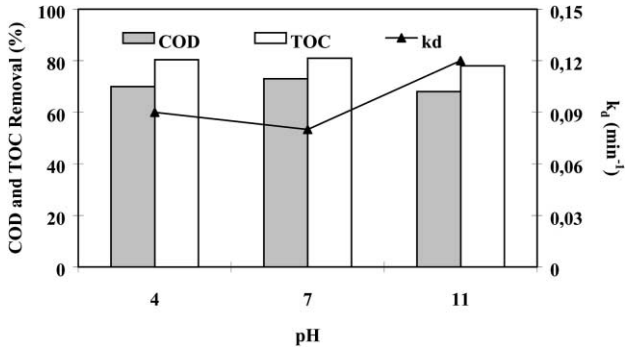

Fig. 5. Changes in k_d-values, overall percent COD and TOC removal efficiencies obtained for 1 g l^{-1} TiO_2/UV-A oxidation of 75 mg l^{-1} waste RB5 in the photocatalytic reactor as a function of pH.

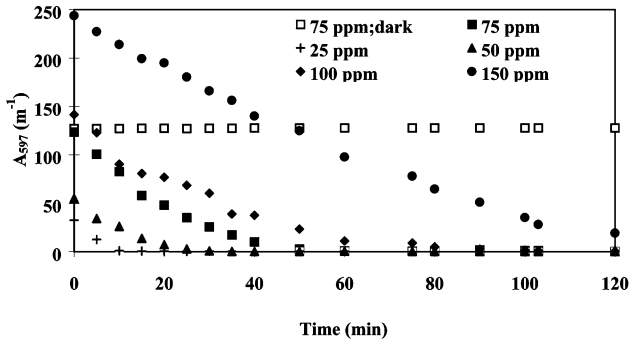

Fig. 6. Time-dependent changes in color during TiO_2/UV-A oxidation of waste RB5 in the photocatalytic reactor at pH 4 at varying initial dyestuff concentrations.

mum amount of dye adsorbed corresponding to monolayer coverage, K, the Langmuir adsorption constant, and R_L, the separation factor. From the data in Fig. 4 it is obvious that adsorption of 75 mg l^{-1} RB5 on TiO_2 at pH 4 was fairly good.

Adsorption studies were also conducted at neutral (7) and basic pH-values (9 and 11). It was observed that increasing the pH resulted in a drastic decrease in the adsorption of the anionic azo dye on TiO_2 to insignificant levels at neutral and basic pH. Due to the fact that the zero-point-of-charge of TiO_2 (TiO_{2ZPC}) lies at pH 6.3 [32,34] it is reasonable to expect that adsorption on and repel from the TiO_2 surface will depend on the electrical charge of the dye and the photocatalyst surface.

3.2.2. Effect of pH

The effect of pH on the heterogeneous photocatalytic oxidation of 75 mg l^{-1} hydrolyzed RB5 has been examined at pH 4, 7 and 11 and the obtained results are presented in Fig. 5 in terms of removal in the selected environmental parameters (COD, TOC) and first order decolorization rate constants (k_d).

As apparent in Fig. 5, percent overall COD and TOC removal efficiencies were similar for each reaction pH ranging between 68–73 and 78–81%, respectively, while the decolorization rate was appreciably faster at pH 11 (k_d = 0.12 min^{-1} instead of 0.09 and 0.08 min^{-1} at pH 4 and 7, respectively). Although the decolorization rate was rather insensitive in the pH range 4–7, it increased significantly beyond pH 11.0. This is probably due to the chemisorptive properties of TiO_2 and/or the different photoreaction mechanisms observable at varying pH. Assuming that the photocatalytic degradation proceeds mainly via $OH^\bullet$ attack at higher pH-values, and via valence band hole (h_{vb}^+) oxidation at acidic and neutral pH, it is expected that decolorization is favored at alkali pH, where the photocatalyst surface is highly hydroxylated. An abrupt acceleration in decolorization kinetics at pH > 11 was also observed for the ozonation of spent reactive dye-bath liquors at different pH-values in a previous work [12].

However, since this difference in reaction rates could not be observed for COD and TOC abatement rates, it might be inferred that similar intermediate oxidation products were formed at the whole investigated pH range which lead to close ultimate oxidation performances.

3.2.3. Effect of initial dyestuff concentration

The photocatalytic decolorization of RB5 in the presence of 1 g l^{-1} suspended TiO_2 was examined in the 25–150 mg l^{-1} initial dye concentration range at pH 4 for 2 h (Fig. 6). RB5 and TiO_2 suspensions were pre-equilibrated for 80 min prior to the photocatalytic reactions.

Comparison of the decolorization curves displayed in Fig. 6 clearly show that an increase in the initial dye concentration from 25 to 150 mg l^{-1} at pH 4 leads to decreased decolorization rates. By increasing the initial RB5 concentration from 25 to 100 mg l^{-1}, the k_d-values abruptly decreased from 0.303 to 0.049 min^{-1}. However, at an initial azo dye concentration of 150 mg l^{-1}, decolorization kinetics changed to zero order (k_d = 2.05 or 1.19 mg l^{-1} min^{-1}). This behavior clearly revealed that at higher initial dye concentrations such as 150 mg l^{-1}, the reaction rate is rather limited by the concentration of oxidants, namely $OH^\bullet$ produced on the TiO_2 surface. The kinetic trend observed for RB5 can be described by the Langmuir–Hinshelwood (L–H) model, where at high concentrations the reaction rate approaches zero order with respect to the initial dye concentration and, in contrast, for concentrations below a certain value (in the present study <150 mg l^{-1}), the reaction rate will appear to be first order with respect to the dye concentration. The following kinetic equation can be used as a good approximation over a wide range of initial pollutant concentrations [35]:

$$-\ln\left(\frac{A}{A_i}\right) = k_r K t = k_d t \quad (6)$$

where k_r is the photocatalytic reaction rate constant, K the equilibrium adsorption constant and k_d the apparent (pseudo-first order) decolorization rate constant with $k_r K = k_d$. In the case that obtained k_d-values decrease with

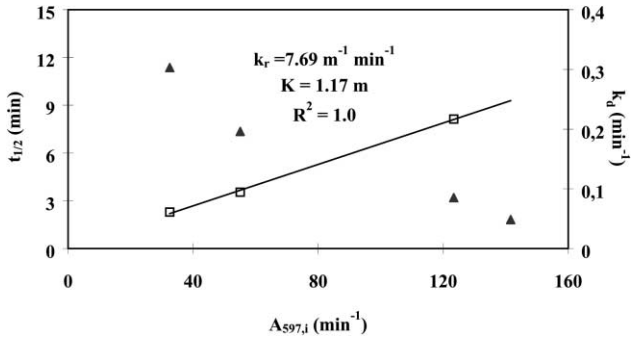

Fig. 7. The modified Langmuir–Hinshelwood plot and kinetic constants obtained for TiO_2/UV-A treatment of waste RB5 in the photocatalytic reactor at pH 4.

increasing initial absorbance A_i of the dyehouse effluent, the total color abatement rate is the sum of zero order and pseudo-first order decolorization [36,37]:

$$\ln\left(\frac{A}{A_i}\right) + K(A_i - A) = k_r K t \tag{7}$$

In this study, overall decolorization rate constants were used instead of initial reaction rate constants [11] for the calculation of L–H constants. On the basis of the L–H kinetic model transformed into Eq. (7), a linear plot of $t_{1/2}$ (half-life for photocatalytic decolorization) against A_i is obtained:

$$t_{1/2} = \frac{0.693}{k_r K} + \frac{0.5 A_i}{k_r} \tag{8}$$

In Fig. 7, the L–H plot and constants are presented for RB5 dye at pH 4.

The decrease in the photocatalytic decolorization rate at high concentrations can also be explained by the competitive UV-A absorption of the disazo dye and TiO_2. This effect reduced the photoactivity of TiO_2 for the formation of $OH^{\bullet}$.

Table 3 compares Langmuir constants obtained from the dark adsorption tests with the L–H constants obtained from the heterogeneous photocatalytic oxidation experiments conducted with RB5 at pH 4.

According to Table 3, only the adsorption constants (K-values) can be compared for the two kinetic models. The obtained adsorption rate constants are almost identical and this result confirmed that the use of overall decolorization for the calculation of L–H constants was more suitable. Further, considering the separation factor R_L, dark adsorption of RB5 on TiO_2 is favorable at pH 4.

Table 3
Comparison of Langmuir adsorption and Langmuir–Hinshelwood kinetic constants obtained for 25–150 mg l^{-1} RB5 at pH 4

Kinetic constants	Langmuir	Langmuir–Hinshelwood
y_m (mg g^{-1})	31.60	–
k_r (mg l^{-1} min^{-1})	–	4.47
K (l mg^{-1})	1.94	2.01
R_L	5.63×10^{-3}	–

Table 4
Overall treatment performances of the 2 h photochemical and photocatalytic advanced oxidation of RB5 at optimized reaction conditions of the selected AOPs

Type of AOP	k_d (min^{-1})	COD (%)	TOC (%)
H_2O_2 (340 mg l^{-1})/UV-C/pH 7	0.16	61.6	74.9
TiO_2 (1 g l^{-1})/UV-A/pH 4	0.09	80.4 (34.4)[a]	70.0 (32.7)[a]

[a] Removal due to dark adsorption on the photocatalyst.

At higher dye concentrations, larger amounts of dye molecules adsorb on the photocatalyst surface and compete with OH^- and H_2O for photoactive semiconductor surface sites, thus, inhibiting the heterogeneous photocatalytic reaction seriously. This results in the observed decrease in the pseudo-first order decolorization rate constants. In addition, it should also be kept in mind that the incident UV-A quanta can be adsorbed via both TiO_2 and RB5 molecules present in the reaction solution such that the amount of photons reaching the photocatalyst surface is drastically reduced.

Overall treatment performances of the investigated homogenous and heterogeneous AOP at the selected reaction conditions are summarized in Table 4 in terms of k_d-values, COD and TOC removal efficiencies.

Judging from the above considerations and the data presented in Table 4, both AOP techniques seem to be quite promising for the treatment of refractory dyestuffs found in textile industry effluents.

4. Conclusions

Photochemical and heterogeneous photocatalytic oxidation processes based on the use of UV-C and UV-A light sources could be efficiently applied for the degradation of non-biodegradable waste disazo dye RB5 in its hydrolyzed form. Complete decolorization accompanied by substantial reductions in COD (average = 66%) and TOC (average = 78%) with the use of optimal operational parameters. In particular, the following conclusions could be drawn from the experimental results of the present study.

1. Photochemical oxidation via mere UV-C and UV-A light irradiation played a minor role during degradation of hydrolyzed RB5 dye. Varying the reaction pH had a negligible effect on the investigated environmental sum parameters COD and TOC whereas the decolorization rate constant slightly increased at pH 11–11.5 for both advanced oxidation systems.
2. For the H_2O_2/UV-C treatment of 75 mg l^{-1} RB5 solution at pH 7, an optimum dose of 10 mM (340 mg l^{-1}) H_2O_2 was found to give a decolorization rate constant of only 0.155 min^{-1} and an overall COD and TOC removal rate of 62 and 75% after 2 h oxidative treatment, respectively.
3. Beyond the critical H_2O_2 dose, the oxidation rate first reached a plateau at 25 mM and decreased slightly at elevated doses ($\geq$50 mM). The shape of the applied

H_2O_2 dose–RB5 degradation curve followed an oxidant dose–pollutant removal rate trend being typical for the H_2O_2/UV-C processes. However, the optimum H_2O_2 dose is pollutant-specific and, thus, has to be determined separately for each treatment case.

4. Pre-equilibration adsorption of RB5 on the TiO_2 photocatalyst surface was achieved after 80 min treatment in the dark adsorption period as a consequence of the electrostatic repulsion between the positively charged TiO_2 and the anionic reactive dye at acidic pH. The initial dark adsorption of 75 mg l^{-1} RB5 accounted for 27.7% color, 34.4% COD and 32.7% TOC removal.
5. Separate dark adsorption tests revealed that 75 mg l^{-1} RB5 adsorption on 0.25–2.00 g l^{-1} TiO_2 at pH 4 could be successfully modeled by the Langmuir adsorption equation with the characteristic constants obtained as $K = 1.94\,l\,mg^{-1}$ and $y_m = 31.60\,mg\,g^{-1}$.
6. Degussa P25 TiO_2-mediated photocatalytic degradation of 75 mg l^{-1} RB5 at pH 4 proceeded relatively slow ($k_d = 0.09\,min^{-1}$; pH 4) and color removal was complete only after 1 h treatment. Overall COD and TOC removal rates obtained for 2 h photocatalysis of 75 mg l^{-1} RB5 were found as 80.4 and 70.0%, respectively at the same pH.
7. It was also established that increasing the RB5 concentration decreased the pseudo-first order decolorization rate constant dramatically and the data could be successfully fitted to the empirical L–H equation with $K = 2.01\,l\,mg^{-1}$ and $k_r = 4.47\,mg\,l^{-1}\,min^{-1}$ at a concentration range of 25–100 mg l^{-1} RB5 and the presence of 1 g l^{-1} TiO_2 at pH 4.

Acknowledgements

This study was a part of Project no. 98Y-03, that is financially supported by Bogaziçi University Research Fund.

References

[1] A. Reife, T. River, H.S. Freeman, Pollution prevention in the production of dyes and pigments, Text. Chem. Col. Am. Dyst. Rep. 32 (2000) 56.
[2] A. Reife, D. Betowski, H.S. Freeman, Dyes and pigments, environmental chemistry, in: R.A. Meyers (Ed.), Environmental Analysis and Remediation, Wiley, New York, 1998.
[3] A. Reife, S. Freeman, Environmental Chemistry of Dyes and Pigments, Wiley, Canada, 1996.
[4] P.C. Ho, Environ. Sci. Technol. 20 (1986) 260.
[5] W.H. Glaze, J.W. Kang, D.H. Chapin, Oz. Sci. Eng. 9 (1987) 335.
[6] D.W. Sundstrom, B.A. Weir, H.E. Klei, Environ. Prog. 8 (1989) 6.
[7] F.J. Benitez, J. Beltran-Heredia, J.L. Acero, T. Gonzalez, Toxicol. Environ. Chem. 47 (1995) 141.
[8] W.H. Glaze, Y. Lay, J.W. Kang, Ind. Eng. Chem. Res. 34 (1995) 2314.
[9] S.E. Law, J. Wu, D.R. Hitchcock, M.A. Eitemann, in: Proceedings of the International ASAE Meeting, Phoenix, Arizona, 1996.
[10] M.L. Marechal, Y.M. Slokar, T. Taufer, Dyes Pigments 33 (1997) 181.
[11] I. Arslan, I.A. Balcioglu, Dyes Pigments 43 (1999) 189.
[12] I. Arslan, I.A. Balcioglu, T. Tuhkanen, Chemosphere 39 (1999) 2767.
[13] N.H. Ince, D.T. Gönenç, Environ. Technol. 18 (1997) 179.
[14] Calgon Carbon Oxidation Technologies, The AOT Handbook (London), Ontario, 1995.
[15] W.G. Kuo, Water Res. 26 (1992) 881.
[16] E.G. Solzhenko, N.M. Soboleva, V.V. Goncharuk, Water Res. 29 (1995) 2206.
[17] I.A. Balcioglu, I. Arslan, Environ. Technol. 18 (1997) 1053.
[18] T. Wei, C. Wen, J. Photochem. Photobiol. A: Chem. 69 (1992) 241.
[19] O. Legrini, E. Oliveros, A.M. Braun, Chem. Rev. 93 (1993) 671.
[20] DyStar, Hoechst Corporation, Private communication, Istanbul, Turkey, 1997.
[21] J.R. Easton, The dye maker's view, in: P. Cooper (Ed.), Color in Dyehouse Effluent, The Society of Dyers and Colorists, Alden Press, Oxford, 1995, pp. 6–21.
[22] J. Shore, Cellulosics Dyeing, The Society of Dyers and Colorists, Alden Press, Oxford, 1995.
[23] I. Nicole, J. De Laat, M. Dore, J.P. Duguet, C. Bonnel, Water Res. 24 (1990) 157.
[24] C.G. Hatchard, C.A. Parker, Proc. R. Soc., Lond. A235 (1956) 518.
[25] APHA/AWWA/WPCF, Standard Methods for the Examination of Water and Wastewater, 17th Edition, American Public Health Association, Washington, DC, 1989.
[26] W. Chu, C.W. Ma, Chemosphere 37 (1998) 961.
[27] H.Y. Shu, C.R. Huang, M.C. Chang, Chemosphere 29 (1994) 2597.
[28] C. Walling, S.I. Kato, J. Am. Chem. Soc. 96 (1974) 133.
[29] V. Buxton, C.L. Greenstock, W.P. Helman, A.B. Ross, Phys. Chem. Ref. Dat. 17 (1988) 513.
[30] M. Anbar, P. Neta, Int. J. Appl. Radiat. Isotopes 16 (1967) 493.
[31] C.J. Martino, P.E. Savage, Environ. Sci. Technol. 33 (1999) 1911.
[32] D.F. Ollis, Process economics for water purificaiton: a comparative assessment, in: M. Schiavello (Ed.), Photocatalysis and Environment: Trends and Applications, NATO ASI Series C: Mathematical and Physical Series 237, Kluwer, London, 1988, pp. 663–667.
[33] W.J. Weber, Physicochemical Processes for Water Quality Control, Wiley-Interscience, New York, 1972.
[34] P.C. Heimenz, Principles of Colloid and Surface Photochemistry, Marcel Dekker, New York, 1986.
[35] D.F. Ollis, Environ. Sci. Technol. 19 (1985) 480.
[36] H. Al-Ekabi, N. Serpone, J. Phys. Chem. 92 (1988) 5726.
[37] R.W. Matthews, Water Res. 24 (1990) 653.